# Low-cost interference lithography

Corey P. Fucetola,<sup>a)</sup> Hasan Korre, and Karl K. Berggren Research Laboratory of Electronics, Massachusetts Institute of Technology, Cambridge, Massachusetts 02139

(Received 2 July 2009; accepted 14 September 2009; published 3 December 2009)

The authors report demonstration of a low-cost ( $\sim 1000$  USD) interference lithography system based on a Lloyd's mirror interferometer that is capable of  $\sim 300$  nm pitch patterning. The components include only a 405 nm GaN diode-laser module, a machinist's block, a chrome-coated silicon mirror, substrate, and double-sided carbon scanning electron microscopy (SEM) tape. The laser and the machinist's block were assembled in a linear configuration, and to complete the system, the mirror and substrate were taped to perpendicular surfaces of the machinist's block. Approximately 50 silicon substrates were prepared, exposed, and developed, after which some were inspected in a SEM. The associated laser spectrum was also measured, enabling calculation of the laser's fringe visibility as it varied along the substrate surface. To compare the exposed resist pattern to the fringe visibility, the authors measured the first order diffraction efficiency as a function of position along the grating surface. Their measurements indicated that artifacts seen in both the optical spectrum and resulting grating patterns arose from the laser diode source, thus improving the source characteristics will be the topic of future work. © 2009 American Vacuum Society. [DOI: 10.1116/1.3245990]

# I. INTRODUCTION

Interference lithography (IL) systems generally exist in larger well-equipped laboratories, where their  $\sim$  50 000 USD price tag is not a substantial constraint. These tools are designed to pattern periodic structures over large areas  $(>1 \text{ mm}^2)$  for applications such as spectroscopy, magnetic storage, and nanofabrication process development.<sup>1</sup> However, some of these applications, such as nanofabrication process development, do not require large grating areas. Hence, there also exists a need for  $<1 \text{ mm}^2$  area patterning in a variety of smaller laboratories and educational facilities that is not being met in part due to cost, access, infrastructure, and maintenance requirements of existing IL tools. We demonstrate here a method of IL, costing <1000 USD, capable of  $\sim 300$  nm pitch patterning that uses a 200 USD 405 nm diode laser and simplified setup to improve the accessibility of IL to a broader array of laboratories.

The concept of using 405 nm light from solid-state sources is not new. Some examples of lithography tools that use 405 nm diodes as light sources have recently been reported.<sup>2-4</sup> In 2003, a blue diode laser was used to write 130-nm-wide pits in a read-only memory disk.<sup>2</sup> In 2006, Heidelburg Instruments<sup>3</sup> produced a 1  $\mu$ m linewidth direct-write diode-laser-based pattern generator. In 2008, an UV-light emitting diode optical-projection lithography system capable of 2  $\mu$ m linewidth was presented in the 34th Micro and Nano Engineering Conference.<sup>4</sup> However, use of these sources for IL has not been reported.<sup>5</sup>

Figure 1 shows two varieties of a Lloyd's mirror interferometer: a simple optical apparatus that can be used to make controllable-pitch lithographic periodic patterns in a photoresist. While a Lloyd's mirror interferometer is not ideal when the laser has multiple transverse modes, the simplicity of its setup, alignment, and operation made it more accessible to a broader community. In Fig. 1(a), we show a conventional Lloyd's mirror lithography system used to pattern samples with areas larger that  $1 \text{ cm}^2$ , which requires a laser source with adequate temporal coherence length and wavelength under 500 nm, a collimating lens, a spatial filter, a long beam-expansion region, a mechanically rigid rotatable mirror, and sample holder. In Fig. 1(b), we show the simplified version that uses only the essential elements, sufficient for  $\sim 1 \text{ mm}^2$  area patterning. This version uses only an inexpensive 405 nm diode laser with a machinist's block used to hold the mirror and sample. The only optical elements in this tool are the diode facet and Cr mirror. The core requisite feature of the interferometer, that it generates subwavelength optical patterns, is retained in both approaches.

In this article, we demonstrated a simple 405 nm diode laser and optical apparatus able to pattern small areas with 300 nm pitch patterns. The diffraction gratings produced by this tool had nonuniformities—visible to the naked eye—due to nonidealities in the spectrum of the diode. Despite these nonuniformities, this tool was capable of printing millimeterscale diffraction gratings with subwavelength periodicity. Notably, the capital cost of the tool was less than 1000 USD.

# **II. APPARATUS AND PROCEDURES**

The demonstration required a combination of new equipment development (the Lloyd's mirror itself), process development for the lithography work, and metrology and evaluation (of the laser source, and the resulting patterned samples). The metrology of the laser source consisted simply of power and spectral characterization, while the samples

<sup>&</sup>lt;sup>a)</sup>Electronic mail: corey.fucetola@mit.edu

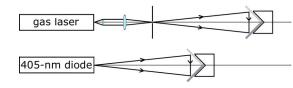


FIG. 1. (Color online) Two configurations of the Lloyd's mirror lithography system: (a) includes a collimated, long coherence length source and spatial filter upstream of the mirror/substrate chuck to improve the beam quality and (b) includes both an inexpensive 405 nm diode laser and an inexpensive mirror/substrate chuck. In (a), the mirror/substrate chuck holds both a mirror and substrate in a perpendicular orientation, which can be rotated to control the pattern pitch. In (b), the same configuration is chosen but the chuck is fixed, the spatial filter is removed, and the gas laser is replaced by a 405 nm diode laser. The distance between the laser and stage was  $\sim$ 25 cm; the mirror was  $2 \times 4$  cm<sup>2</sup> and the substrates were quarter wafers approximately 8-12 cm<sup>2</sup> in area.

were characterized by electron microscopy and by determining the spatial distribution of diffraction efficiency across the sample by using a custom-built apparatus.

Figure 1(b) shows a schematic view of a Lloyd's mirror interferometer used for lithographic exposure, consisting of (1) an optical source and (2) a machinist's block. The source consisted of a 5 mW 405 nm wavelength diode laser module, which was  $\sim 5 \times$  cheaper than a single-mode diode. The source was aligned using a collimating lens and a prism polarizer cut at the Brewster angle to set the incident polarization at the mirror and sample to s polarization, or equivalently, the electric field was set perpendicular to the mirror's plane of incidence (and hence parallel to the grating lines). The polarizer and lens were then removed prior to sample exposures so that the elliptically shaped, diverging light emitted from the diode had the short axis of the ellipse aligned parallel to the grating lines. The machinist's block held a mirror consisting of a silicon wafer coated by electron-beam evaporation with 25 nm of chrome on one of its faces, mounted with two-sided adhesive carbon tape. The mirror's reflectivity was measured for 45° incident, s-polarized, light to be 76.5%. On the perpendicular face, the block held the sample, also mounted with two-sided adhesive carbon tape, so that the edge of the sample was nested behind the mirror edge. The block was separated from the source by  $\sim 25$  cm.

Because the laser spectrum can influence the fringe visibility in the interferometer, we used a spectrometer to record the optical output spectrum of the laser prior to exposing samples. The spectrum was measured using a Spectrex spectrometer with 5.5 pm spectral resolution. Since the spectrum was found to drift with use, the lasers were not used for other purposes between the spectrum measurement and the exposure (although the time lag between measurement and exposure varied between samples from a few hours to a few weeks). While there are a variety of ways<sup>6</sup> to stabilize the spectrum emitted by the diode, including optical, mechanical, thermal, and electrical feedback, it was not necessary to introduce these methods to achieve good results during this initial demonstration.

We developed a standard process for the samples consist-

2959

ing of application of a trilayer resist stack, optical exposure, and development. 75 and 100 mm wafers were coated with a resist stack' consisting of three separate layers: (1) an antireflection coating (ARC) (AZ Electronic Materials, Barli) applied by spin coating at  $\sim$ 7.28 krpm to achieve a 200 nm thickness, followed by baking on a hot plate at 175 °C for 90 s, (2) 25 nm of SiO<sub>x</sub> sublimated in an electron-beam evaporation system with deposition thickness controlled using in situ quartz crystal monitor, and (3) a positive-tone photoresist (PFI-88, Sumitomo Chemicals) spin coated at  $\sim$ 3.8 krpm to achieve an estimated thickness of  $\sim$ 180 nm and then baked on a hot plate at 110 °C for 90 s. The SiO<sub>x</sub> interlayer is incorporated into the resist stack for postlithographic processing, wherein it masks the ARC during subsequent etch transfer steps. After deposition of the  $SiO_x$  but before application of the photoresist, wafers were coated with a layer of hexamethyldisilazane (HMDS) by spin coating using the following procedure: (1) application of  $\sim 30$ drops of HMDS from a plastic pipette to coat the sample surface, (2) a delay of 60 s, (3) 5 s spinning at  $\sim$ 3.8 krpm, and (4) delay in ambient environment of  $\sim 5$  min before further processing to permit the surface to fully dry. After application of photoresist, the wafers were cleaved into quarters, forming  $\sim 8-12 \text{ cm}^2$  pieces used for individual exposure experiments. Optical dose was controlled by using a simple shutter to unblank the optical beam for a timed period. Typical exposure times were  $\sim 25-30$  s, and the optical power was  $\sim$ 5 mW. Samples were developed by liquid immersion in 0.26N (2.4% wt) tetramethylammonium hydroxide developer (CD-26, Rohm & Haas Electronic Materials) for 60 s, then rinsed also by immersion in de-ionized water, and finally blown dry using dry N<sub>2</sub> gas.

After processing, samples were inspected visually with the naked eye, and then briefly in an optical microscope to verify the presence or absence of a grating, but then inspected closely by scanning-electron microscopy (SEM). The SEM was calibrated by using an image of a standard grating. Prior to SEM inspection, samples were coated by sputter deposition of <5 nm of Au/Pd. The scanningelectron microscope imaging was performed on a DSM 982 Gemini SEM column from Zeiss SMT, with an in-lens secondary-electron detector, at 5 keV with a 7 mm working distance.

In addition to imaging, samples were evaluated by using a custom-built apparatus to determine the variation in diffraction efficiency across the sample. In this experiment, the fabricated sample was placed on a linear translation stage and illuminated with a 405 nm optical beam with a diameter of 82  $\mu$ m at the substrate. The sample was aligned so that the grating lines were perpendicular to the direction of stage motion and to the laser's plane of incidence. A power meter was then placed in the path of the first-order diffraction spot. The reading on the power meter was recorded as a function of stage position in order to determine position dependence of the diffraction efficiency across the sample.

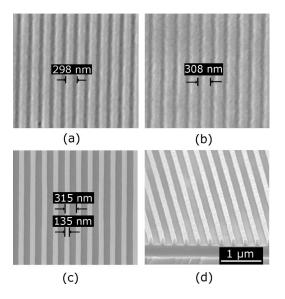


FIG. 2. Three exposures with different doses and spectra, taken on three different days, separated by several weeks. Note that the incident angles,  $\theta_a$ ,  $\theta_b$ ,  $\theta_c$ , in the three images varied slightly from run to run, but could be calculated from the period of the gratings shown in (a), (b), and (c). The associated periods and the known wavelengths for each sample can then be used to determine the angle of incidence of the laser on the surface. (d) is the cross section of the grating shown in (c).

#### **III. RESULTS AND ANALYSIS**

Throughout the course of this work, 45 samples were exposed and developed. Many of these samples resulted in grating structures, but we focused on three, in particular, (a), (b), and (c), because in these cases we had measured the spectrum of the laser immediately prior to these exposures. These samples were characterized by optical inspection and microscopy, electron microscopy, and diffraction-efficiency mapping as discussed above.

Figure 2 shows the SEM images of patterned regions of each of the three samples [(a), (b), and (c)] and corresponding measurements of the grating periods. SEM images confirmed qualitative evaluation of the gratings: gratings (a) and (c) exhibited superior diffraction quality upon visual inspection under normal ambient room illumination, while grating (b) required inspection in bright light (ideally full sunlight). Furthermore, they provided a precise measurement of the grating period [298, 308, and 315 nm for gratings (a), (b), and (c) respectively]. We hypothesize that the observed variance of a few percent in grating period was due to variation in alignment of the laser and machinist's block from run to run.

Assuming that the variance in grating period was due to a corresponding variance in the angle of incidence of the laser on the substrate, we determined this angle by using the SEM-measured grating periods. The period  $p_i$  can be related to the half-angle of the interfering beams  $\theta_i$  (which can vary slightly depending on the configuration of the machinist's block or alignment of the laser) by the formula

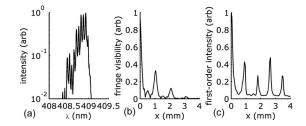


FIG. 3. Analysis of one of the gratings that was exposed with  $0.728 \text{ mW/cm}^2$  at the resist surface for 22 s. (a) The laser spectrum, measured before the exposure for the sample shown in Fig. 2(a). (b) Calculated fringe visibility projected onto the wafer surface. The incident angle during the exposure was calculated from Eq. (1) and used to project the fringe visibility onto the surface of the substrate through Eq. (3). (c) Measured first order diffracted power from the grating. The first order diffracted power was normalized over the interval from 0 to 1.

$$p_i = \frac{\lambda_i}{2\sin\theta_i},\tag{1}$$

where *i* is the corresponding sample index, *a*, *b*, or *c*, and  $\lambda_i$  is the wavelength at the peak of the optical spectrum. The measured period for each sample and average wavelength for that exposure was used in conjunction with Eq. (1) to establish the half-angle between the two interfering beams. For  $p_a=298$  nm,  $p_b=308$  nm, and  $p_c=315$  nm, and  $\lambda_a=\lambda_b=408.8$  nm and  $\lambda_c=408.7$  nm (the peaks of the measured laser spectra in each case), the angle corresponds to  $\theta_a=43.3^\circ$ ,  $\theta_b=41.6^\circ$ , and  $\theta_c=40.4^\circ$ . The observed variance of a few degrees is consistent with the care taken in alignment of each sample (which was performed by eye).

As discussed earlier, diffraction efficiency (and pattern quality) varied greatly across samples on the length scale of millimeters. We hypothesize that this variance was associated with the imperfect temporal coherence of the source. To support this hypothesis, we compared the measured spatial distribution of diffraction efficiency to the calculated fringe contrast based on the measured source spectrum. The fringe contrast can be calculated [by using the measured source spectrum and the relationship given by Eq. (1)] as a function of grating position by using the equation

$$V(\Delta L) \propto \int_0^\infty I(\nu) e^{-i2\pi\nu\Delta L/c} d\nu,$$
(2)

where  $\Delta L$  is the optical path difference between the two arms of the interferometer.<sup>8</sup> The optical path difference can be related to the distance x from the intersection of the mirror with the sample surface by using the equation

$$x = \Delta L \frac{\sin \theta}{(1 + \cos(\pi - 2\theta))}.$$
(3)

Figure 3 shows the impact of the laser spectrum on the diffraction efficiency of the final grating: the spectrum was measured, used to calculate the fringe visibility distribution, and then compared to the measured diffraction efficiency. Figure 3(a) shows the measured laser spectrum prior to exposing the sample shown in Fig. 2(a). Figure 3(b) shows a calculation of the expected fringe visibility versus position

on the substrate, calculated using the laser optical spectrum shown in Fig. 3(a). Finally, Fig. 3(c) shows the measured diffraction efficiency. Notice the recurrence of regions with strong diffraction visibility observed, and predicted from the calculated result in Fig. 3(b). We interpret this recurrence as being due to the beating of distinct power peaks in the optical spectrum.

## IV. DISCUSSION AND SUMMARY

Inexpensive 405 nm diode lasers do have some limitations that need to be addressed in order to improve the system performance. Generally, they are multimode, and as a result exhibit poor spatial and temporal coherences. Also, the output power from these inexpensive 405 nm laser diodes is not controlled via feedback with a photodiode.<sup>6</sup> These limitations will restrict the extent and stability of an interference pattern; however, despite these challenges the use of 405 nm diode-laser sources can still be of practical use for IL.

The key to realizing cm<sup>2</sup> or larger patterning areas in future work is primarily improving the coherence length of the source. This can be simply accomplished either by purchasing single-mode sources (which currently are available for  $\sim 2000$  USD) or by suppressing additional modes by using optical feedback from an external cavity. These approaches will be the subject of future work.

Beyond improving both the spatial and temporal coherences of the source, additional improvements to the repeatability of the grating pitch could in principle be accomplished through more precise alignment of the substrate stage to the optical axis of the laser. For the system shown in Fig. 1(a), Walsh<sup>1</sup> described the tolerance on the positioning of the substrate chuck relative to its rotation and translation from the optical axis of the laser. Currently, we have made no provision to align the chuck relative to the optical axis with better precision than  $\sim 1/2$  mm of translation. In addition to discussing the alignment technique, in Ref. 1 is also an indepth discussion of both the stability and repeatability of the interference pattern generated by a Lloyd's mirror.

To this point, we have focused on construction and utilization of the IL tool and have not described the design of the substrate resist system that would be most suitable for process development. While simple designs are preferred, the ideal photoresist structure for process development is a dense pattern that has a resist lines with rectangular cross section. This type of profile can be achieved in resist when the thickness of the ARC layer between the substrate and resist is chosen appropriately to reduce undesired optical interference in the resist. This interference arises from reflections of the incident light as it crosses the material interfaces beneath the photoresist. These reflections are collectively referred to as the back reflectance into the photoresist. If the back reflectance is not suppressed,<sup>7</sup> it will cause an additional standing wave to develop in the vertical walls of the grating. After development, this standing wave can then be transferred during subsequent processing steps, so reducing its amplitude is important. Fortunately, algorithms exist<sup>9</sup> that can be used to design the thickness of an ARC layer to reduce these back reflections. Using one of these, an ARC thickness (~200 nm for our setup) can be chosen to reduce the back reflectance to as low as 1% or 2%.

The key result of this article was the demonstration of  $\sim$  300 nm pitch patterning capability at low cost. For less than 1000 USD, we were able to print grating lines with our Lloyd's mirror. The capabilities and accessibility of this tool suggest that 405 nm diode lasers could be used as sources for IL in both laboratory and educational settings.

### ACKNOWLEDGMENTS

The authors would like to acknowledge Tim Savas and Thomas O'Reilly for their helpful discussions about the diffraction grating artifacts, Jeremy Johnson for his help in measuring the optical spectrums, and Maria Csete for her help in setting the polarization of the interferometer. Funding for this project was provided by the Singapore-MIT Alliance.

- <sup>2</sup>A. Kouchiyama, K. Aratani, Y. Takemoto, T. Nakao, S. Kai, K. Osato, and K. Nakagawa, Jpn. J. Appl. Phys., Part 1 42, 1794 (2003).
- <sup>3</sup>Heidelburg Instruments, http://www.himt.de/factsheets/muepg101.pdf (downloaded June 16, 2009).
- <sup>4</sup>C. C. Su, T. C. Wu, J. H. Hsu, S. J. Hwang, and S. H. Chang, in Proceedings of the 34th Micro and Nano Engineering Conference, Greece, 2008 (unpublished).
- <sup>5</sup>David Tanenbaum (personal communication). We've recently become aware that other groups are using 405 nm diode lasers as sources for IL.
- <sup>6</sup>C. E. Wieman and L. Hollberg, Rev. Sci. Instrum. **62**, 1 (1991).

- <sup>8</sup>J. Goodman, *Statistical Optics*, Wiley Classics Library ed. (Wiley, New York, 2000), pp. 158–164.
- <sup>9</sup>M. G. Moharam, D. A. Pommet, E. B. Grann, and T. K. Gaylord, J. Opt. Soc. Am. A **12**, 1077 (1995).

<sup>&</sup>lt;sup>1</sup>M. Walsh, Ph.D. thesis, MIT, 2004.

<sup>&</sup>lt;sup>7</sup>M. L. Schattenburg, R. J. Aucoin, and R. C. Fleming, J. Vac. Sci. Technol. B **13**, 3007 (1995).